

POWER ELECTRONICS SYSTEM FOR SOLAR ENERGY SUPPLY OF PUBLIC LIGHTING DURING PEAK DEMAND

Edilson Mineiro Sá Jr., Sérgio Daher, Cícero Cruz and Fernando Antunes

Federal University of Ceara

Department of Electrical Engineering

Group of Processing of Energy and Control–GPEC

P. O. BOX 6001 – Campus of the Pici – 60455-760 – Fortaleza – CE - Brazil

edilson@dee.ufc.br

Abstract–This work presents the development of the photovoltaic system for energy supply to the public illumination in peak demand in electric system distribution. The system can supply energy, considering a solar radiation average of 5500W/m²/day, for two and a half hours, to a 70W high-pressure sodium lamp (HPS). During the day, the solar energy is captured by a photovoltaic panel and stored in lead acid batteries through a boost converter. This converter makes possible the battery to be charged in photovoltaic maximum power point (MPP). In the evening the HPS lamp is started up through an electronic ballast, which operates with zero volt switch (ZVS). The system, controlled by a AT90S8535 RISC microcontroller, seeks the photovoltaic maximum power point, monitors the batteries level and determines the time operation of the DC/DC converter, that makes possible the use of the electronic ballast with the batteries.

I. INTRODUCTION

A photovoltaic system cost is thoroughly related with what is considered cost and what is considered benefit. Being taken the market prices and the cycle of life of a photovoltaic system, the cost of the generated electricity can be around 0,30 to 1,00 USD/kW. This cost has been limited factor in the use of photovoltaic systems in comparison with costs for electric energy from hydraulic, nuclear or fossil source. Considering, however, the difficulties that today are imposed in the construction of new generation plant, the difficulties and cost in the construction of new transmission lines, factors as more expensive energy in the hours of demand peak and the deregulation of the electric sector that it makes possible the purchase of energy produced in excess by the photovoltaic system, the proceeding electric power for photovoltaic systems can already be considered economically viable.

For amortization of the initial investments, is very important that the maximum of power can be extracted from the photovoltaic panel. The photovoltaic panel power changes with the temperature, solar radiation and the load. For a efficient it is necessary the use of a microcontroller, together with the power electronics, to adjust the dynamics electric impedance of the photovoltaic panel.

This paper describes the implementation of a photovoltaic system for public illumination, different from other conceptions of self-sufficient systems [1,2,3], this is interlinked the electric net. The energy supplies system, through the batteries, a 70W lamp HPS for two and a half hours, time in that happens the demand peak in the electric system.

A boost converter charges the lead acid batteries, which control is provided by a microcontroller AT90S8535 of Atmel™. The battery is charged at the photovoltaic panel maximum power point. In the evening, the system uses the photovoltaic panel as a light sensor and turns on the flyback DC/DC converter. The electric grid is softly disconnected, due to the high voltage of the dc-dc converter, and energy stored in the batteries supplies the lamp through the ballast for a period of time of two and a half hours. The output of the DC/DC converter is connected directly in the DC link of the electronic reactor. The half bridge circuit of the electronic ballast and the igniter circuit, turn on the lamp.

The diagram in system blocks can be seen in the figure 1. This system is divided in four subsystems directly controlled by the microcontroller: electronic reactor (ballast); the DC/DC converter; the battery charger controller and power factor correction (PFC) stage.

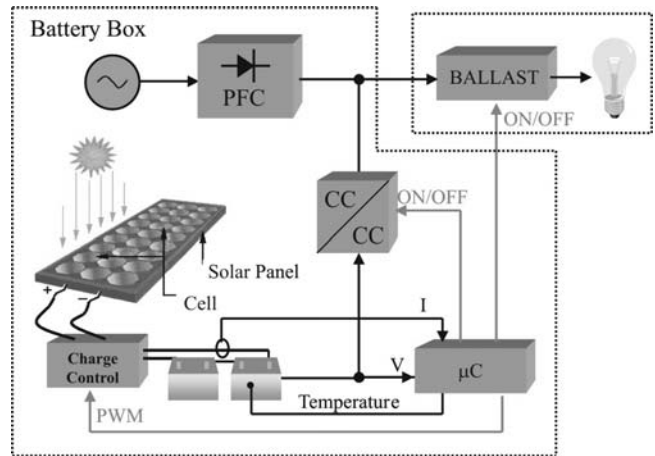


Fig. 1–Diagram in blocks of the developed system.

II. SIZING OF THE PHOTOVOLTAIC MODULES AND BATTERIES

For the design the numbers of the photovoltaic panels and the batteries, the system can be simplified [4].

The average power that should be supplied by the batteries bank during the system operation is defined by the equation 1.

$$P_{Bat} = \frac{P_{out}}{\eta} \quad (1)$$

$P_{Bat} \rightarrow$ Average power supplied by the batteries bank.

η → System efficiency.

P_{out} → Power drained by the load.

The consumption of the system in amperes hour per day (Ah/day) it is defined by the equation 2.

$$Ah_L = \frac{P_{Bat} \cdot t_{func}}{V_{DC}} \quad (2)$$

Ah_L → Daily consumption of the load.

t_{func} → Time of operation of the load a day (h/day).

V_{DC} → Voltage of the battery link (12V, 24V, etc.).

The average capacity of electrical energy production, in amperes hour per day of each photovoltaic panel of 12V is given by the equation 3.

$$Ah_d = \frac{I_{RS} \cdot R_{med}}{R_s} \quad (3)$$

Ah_d → Energy supplied by the photovoltaic module per day.

R_{med} → Daily radiation average rate at the installation place.

R_s → Solar radiation (1000 W/m²).

I_{RS} → Current supplied by the module for radiation R_s .

The minimum number of photovoltaic panels necessary for the specified energy consumption is given by the equation 4.

$$Np = \frac{Ah_L \cdot V_{DC}}{Ah_d \cdot 12} \quad (4)$$

Ah_L → Capacity of daily consumption of the load.

The total capacity of the batteries necessary for operation of the system is given by the equation 5.

$$C_{bat} = \frac{Ah_L \cdot d \cdot V_{DC}}{Dc \cdot V_{bat}} \quad (5)$$

C_{bat} → Total capacity of the batteries.

d → Autonomy days.

V_{DC} → Voltage of the batteries link.

Dc → Discharge depth.

V_{bat} → Voltage of the battery.

The product of the current by the time (Ah) usually specifies the battery energy capacity; this characteristic is supplied for 20 hours of uninterrupted operation. Whenever one wants to use the maximum battery potential in a short time interval, it should be applied to the rated Ah an index obtained from the curves supplied by the manufacturer.

For a medium radiation of 5500W/m²/day in Fortaleza-Ceará-Brazil, 2.5 hours of operation, system efficiency of 80%, lamp HPS 70W, 30% depth of discharge and battery voltage of 24V, two 45Ah stationary batteries were chosen and one 75Wp photovoltaic panel. The batteries used were the model Moura 12MC45 and the 75W photovoltaic panel SiemensTM SP75.

III. THE CHARGE BATTERY CONTROLLER

To maximize the power output from the photovoltaic panel, it should be used algorithms for tracking the maximum power point of the panel (MPPT). For a perfect system design, it is necessary a model for the cell of photovoltaic module [5] This model is shown in figure 2. Being R_s the resistance of the contact metals with the load (fingers) and R_p of the resistances of the crystals of pn junction that constitute the photovoltaic cell.

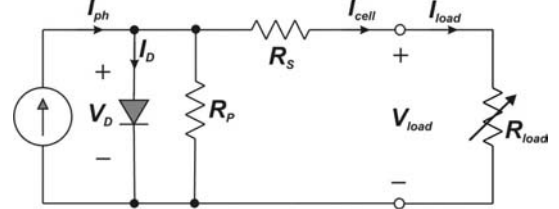


Fig. 2 - The electric model for a photovoltaic cell with load.

The electric model, for the photovoltaic cell can be represented mathematically by the equation 6.

$$I_{cell} = I_{ph} - I_0 \cdot \left(e^{\frac{q}{A \cdot k \cdot T} (V_{load} + I_{cell} \cdot R_s)} - 1 \right) - \frac{V_{load} + I_{cell} \cdot R_s}{R_p} \quad (6)$$

I_{cell} → Cell output current (in A).

I_{ph} → Light-generated current (in A).

I_0 → Cell reverse saturation current or dark current (in A).

q → Electronic charge ($1.6 \cdot 10^{-19}$ C).

V_{load} → Cell output voltage (in V).

A → Ideality constants.

K → Boltzmann's constant ($8.65 \cdot 10^{-5}$ eV/K).

T → Cell temperature (in K).

An association of cells forms the photovoltaic module and its possible circuit representation is showed in figure 3 [6]. Where R_{SM} is the equivalent series resistance, R_{PM} the equivalent parallel resistance of the module, NP number of cells in parallel, NS number of cells in series and I_{phM} the current supplied by the current source of the module.

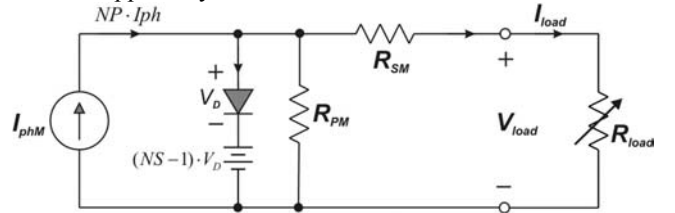


Fig. 3 - The electric model for a photovoltaic module with load.

The manufacturer's manual supplies the maximum current that equivalent the short circuit current (I_{short}), maximum voltage equivalent the open voltage (V_{open}), rated current equivalent the MPP current (I_{MPP}) and rated voltage equivalent the MPP voltage (V_{MPP}). These values are supplied for 1000 W/m² of the solar radiation and temperature of 25°C. Table 1 shows the values for the SP75 module.

Tab. 1 - Electric characteristics of the SP75 Siemens module.

75W SP75 module (Siemens)	
Short circuit current (I_{short})	4,8 A
Open circuit voltage (V_{open})	21,7 V
Rated current (I_{MPP})	4,4 A
Rated voltage (V_{MPP})	17 V

In the maximum power point, considering that R_{PM} is much larger than R_{SM} , the current source of the photovoltaic module (I_{phM}) can be approximate to the maximum current (I_{short}) and the polarization diode voltage (V_D) more the one voltage source to the maximum voltage (V_{open}). The equivalent circuit is shown in the figure 4.

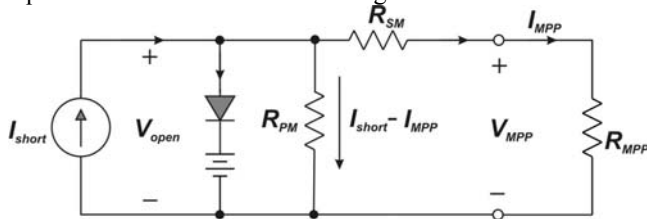


Fig. 4 - Equivalent circuit of the module in the maximum power point.

With the circuit showed in figure 4, the R_{SM} value can be obtained trough the equation 7.

$$R_{SM} = \frac{V_{aberto} - V_{carga}}{I_{MPP}} \Rightarrow R_S = \frac{21,7 - 17}{4,4} \cong 1,068\Omega \quad (7)$$

Similarly, the R_{PM} value can be founded by the equation 8.

$$R_{PM} = \frac{V_{aberto}}{I_{curto} - I_{MPP}} \Rightarrow R_P = \frac{21,7}{4,8 - 4,4} \cong 54,25\Omega \quad (8)$$

The characteristic curve IxV, current versus voltage, obtained through of the ORCAD™ model simulation. This result is presented in the figure 5.

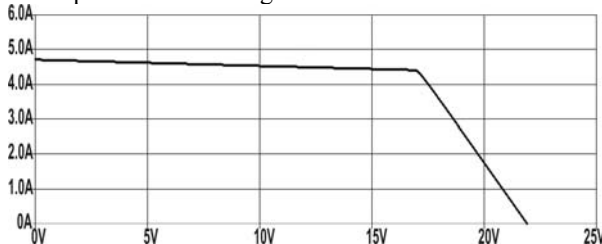


Fig. 5 – The IxV curves of the photovoltaic module obtained by simulation.

The dual behavior can be observed in the photovoltaic module, to the left of the curve as current source and the right as voltage source.

In the figure 6 is presented the PxV curve, current versus voltage, also obtained by simulation.

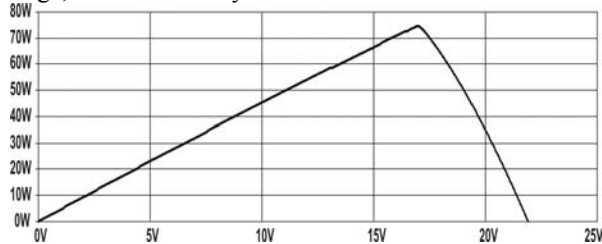


Fig. 6 – Simulated PxV Curve of the photovoltaic module.

Through of the analyze of figures 5 and 6 is observed that the simulated curve is similar to real curve of the photovoltaic module, as showed in the figure 7, what assures the precision of the model.

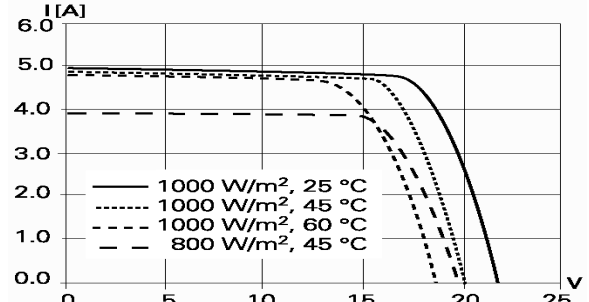


Fig. 7 - The IxV curves of the photovoltaic module, retreat of the manufacturer's manual.

To reduce the current in the converter and minimize the conduction losses, it was used a 24V battery link voltage. However, this voltage required the use of a boost converter for MPPT.

In the maximum power point, the photovoltaic module possesses dual behavior, as current source and voltage source, which makes indispensable the use of a capacitor (C_e) in parallel with the photovoltaic panel. This component, shown in the figure 8, besides guaranteeing that the input of the boost is a voltage source, this makes possible the reduction of the voltage variation in the output of the photovoltaic panel, getting better the MPP tracking.

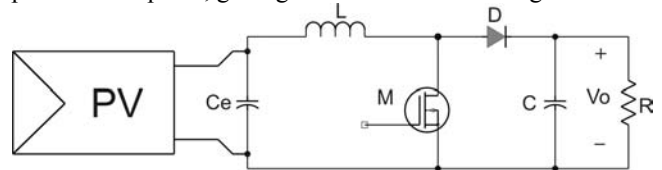


Fig. 8 – The boost converter connected with photovoltaic module and input capacitor.

Considering that all the energy of the current variation is supplied by the capacitor in parallel with the panel (C_e), equation 9 can be obtained.

$$\frac{1}{2} C_e (V_{MAX}^2 - V_{MIN}^2) = \frac{1}{2} L (I_{MAX}^2 - I_{MIN}^2) \quad (9)$$

C_e → Capacitor in parallel with the panel.

V_{MAX} → Maximum voltage in the boost converter input.

V_{MIN} → Minimum voltage in the boost converter input.

L → Boost inductor.

I_{MAX} → Maximum current in the boost converter input.

I_{MIN} → Minimum current in the boost converter input.

In terms of the rated current and its variation, equation 10 is arrived trough equation 9.

$$C_e = \frac{L \cdot I_{NOM} \cdot \Delta I}{V_{NOM} \cdot \Delta V} \quad (10)$$

I_{NOM} → Rated current in the boost input.

ΔI → Current ripple in the boost input.

V_{NOM} → Rated voltage in the boost input.

$\Delta V \rightarrow$ Voltage ripple in the boost input.

The simulate circuit is shown in the figure 9, the boost inductor, L1 is designed for the converter work in continuous conduction.

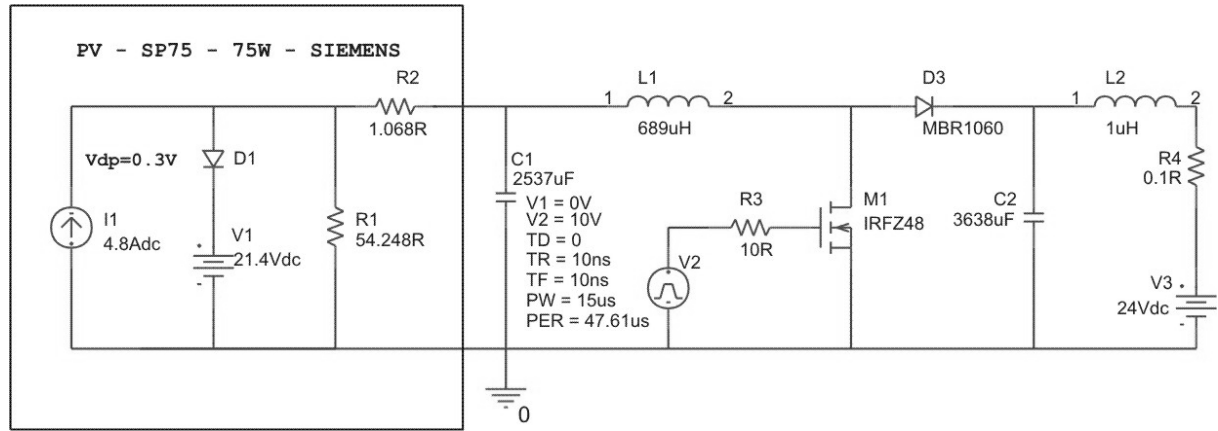


Fig. 9 – Battery charger with the Siemens™ SP75 photovoltaic panel.

The capacitor C1, equivalent to the capacitor C_e , limits the voltage ripple in the panel, as well as guarantees that the input converter is voltage source. The values R1, representing R_{PM} , and R2, representing R_{SM} , they were obtained from the data supplied by the manufacturer's manual. To represent the battery electric cable resistance and its inductance, L2 and R4 were used, that also represents the shunt resistor used with current sensor.

As the battery can be considered as a constant voltage source, It was only necessary to monitor the charge current in the battery [7] to determine the maximum power point and not the input power in the panel, what is usually used [8,9,10]. The battery voltage is also monitored, just to avoid overcharge, what could damage the accumulators.

The power point tracking is similar to the algorithm used by E. Koutroulis [8], but using the battery charge current.

IV. DC/DC CONVERTER

The DC/DC converter used was a flyback converter. This converter makes possible the batteries voltage to set up from 20V or 28V to 311V, the high DC voltage link of the electronic reactor. This converter also makes possible the isolation between the batteries and the electronic reactor, due to its good crossed regulation, the feedback is made by an auxiliary coil.

The CI3524 was used for control, which the microcontroller just enables its operation, turning on or off.

V. THE ELETRONIC BALLAST

The electronic ballast used made possible the direct high DC link connection, It has a high efficiency and a reduced size., when compared to the conventional ballast.

The simplified circuit of the electronic half bridge inverter ballast can be seen in the figure 10. The frequency commutation of the switches is 33kHz. Acoustic resonance was not observed in this value for the lamp model Phillips™ SON 70W [11]. The circuit tank, is formed by L_o and C_c , these components were designed for zero voltage switch (ZVS) operation [12].

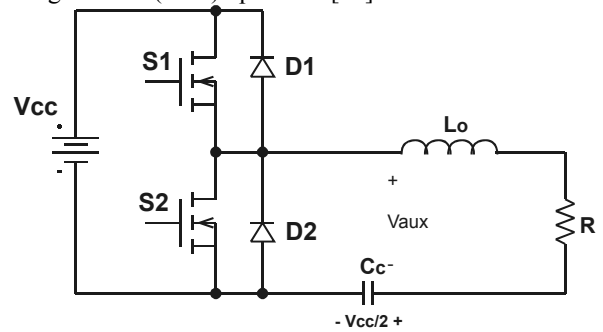


Fig. 10 - The simplified half bridge model for HPS lamp.

The power electronic reactor circuit is shown in figure 11.

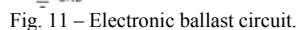


Fig. 13 – Battery charge current (200mA/div).

The figure 16 shows the picture of the developed electronic reactor.

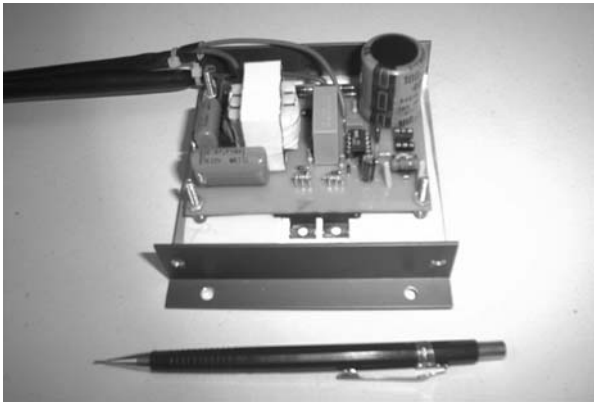


Fig. 16 – Electronic ballast picture.

The figure 17 shows the implemented electronic ballast picture and the HPS lamp in your ignition moment.



Fig. 17 – Ignition moment of the lamp.

VII. CONCLUSIONS

The charge controller, the boost converter used to make the photovoltaic module to work in its maximum power point, was designed and tested through simulations using ORCAD™. This method validated the used circuit and its designer.

The half bridge circuit used made possible the development of a low cost electronic ballast, which was more reduced with the use of the incorporate igniter.

The advanced commutation techniques used, ZVS, made possible the losses reduction and consequently an increment in the circuit efficiency. Another positive point of this technique is the EMI reduction.

VIII. ACKNOWLEDGMENT

Authors wish to thanks the local Electric Energy Utility – COELCE and Ceará State Research Foundation - FUNCAP for financially supporting that research.

IX. REFERENCES

[1] S. R. Harrington and T. D. Hund, "Photovoltaic lighting system performance", *IEEE 25th Photovoltaic Specialists Conference*, May 1996, pp. 1307-1310.

[2] G. Loois, H. de Gooijer, T. van der Weiden and X.Vallvé, "Large scale market introduction of PV public lighting", *2th Word Conference and Exhibition Photovoltaic Solar Energy Conversion*, July 1998, pp. 3107-3110.

[3] N. N. Franceschetti, E. B. Schonward and M. Godoy Simões, "Solar energy based public area illumination system", *COBEP*, vol. 1, 1999, pp. 487-492.

[4] D. C. Martins, M. Mezaroba and I. Barbi, "Treatment of the Solar Energy for a Water Pumping System Using a Current-Fed Parallel Resonant Push-Pull Inverter", *COBEP*, 1999.

[5] C. Hua and C. Shen, "Comparative study of peak power tracking techniques for solar storage system", *Applied Power Electronics Conference and Exposition 1998 - APEC '98*, Conference Proceedings, Thirteenth Annual, vol. 2, 15-19 Feb. 1998, pp. 679-685.

[6] M. Veerachary, T. Senjyu and K. Uezato, "Maximum power point tracking control of IDB converter supplied PV system", *IEE Proc. Electr. Power Appl.*, vol. 148, no. 6, nov. 2001, pp. 494-502.

[7] F. A. Himmelstoss, A. Laimer and A. Brock, "Microcontroller solar battery charge", *2th Word Conference and Exhibition Photovoltaic Solar Energy Conversion*, July 1998, pp. 3127-3130.

[8] E. Koutroulis, K. Kalaitzakis and N. C. Voulgaris, "Development of a microcontroller-based, photovoltaic maximum power point tracking control system", *IEEE Tran. On Power Electronics*, vol. 16, no. 1, Jan. 2001, pp. 46-54.

[9] L. Zhang, A. Al-Amoudi and Yunfei Bai, "Real-time maximum power point tracking for grid-connected photovoltaic systems", *IEE Conf. Power Eletronics and Variable Speed Drives*, Set. 2000, pp. 124-129.

[10] M. F. Shraif, C. Alonso and A. Martinez, "A simple robust maximum power point control (MPPC) for ground photovoltaic generators", *Intern. Power Eletronics Conf.*, 2000, pp. 158-163.

[11] F. S. Cavalcante, "Reatores eletrônicos para lâmpadas de vapor de sódio de alta pressão de 70W" *Dissertação (Mestrado em Engenharia Elétrica) – INEP/EEL*, UFSC, Florianópolis, Dezembro de 2001.

[12] A. Anderson S. "Sistema eletrônico para lâmpadas de descarga de alta pressão para iluminação de exteriores", *Exame de qualificação*, Santa Catarina, Florianópolis, Julho de 2001.